



Structural aspects of ozonides on lymphoma cell viability

Brian Henriksena*¹, Sarah Norris Tysor², Jennifer L. Kopanic² and Richard Lomneth²

¹School of Pharmacy and Health Professions, 2500 California Plaza, Creighton University, Omaha, NE

²Department of Chemistry, University of Nebraska at Omaha, 6001 Dodge St, Omaha NE

ABSTRACT

Artemisinin and its semisynthetic derivatives (1,2,4-trioxanes) are potent antimalarials, and at high concentrations, are also cytotoxic to a variety of cancer cell lines. Synthetic ozonides (1,2,4-trioxolanes) are effective antimalarials that also contain a peroxide pharmacophore, but these compounds have not been tested against cancer cell lines. In this study, we measured the effects of 25 ozonides on Raji lymphoma cell viability using the MTT assay. Eight of the compounds greatly decreased cell viability at 10 μ M while the remainder had limited to no effect. A computational analysis was performed to determine the common structural features of the most active compounds. All of the most active compounds contain an ionizable amine with a narrowly defined distance between the ionizable amine and the trioxolane heterocycle. The fifteen compounds with low activity did not fit these criteria. The two compounds with intermediate activity may form an intramolecular H-bond, effectively reducing their activity against the lymphomas.

Keywords: Malaria, Ozonide, Artemisinin.

INTRODUCTION

Artemisinin is a natural product valued for its medicinal properties, particularly in the treatment of malaria. The compound can be extracted from the Chinese herb *Artemisia annua* L or sweet wormwood that has been used for centuries in China [1]. It is a sesquiterpene lactone containing a 1,2,4-trioxane heterocycle core substructure required for its antimalarial action [2,3]. Synthetic ozonides (1,2,4-trioxolanes) have been developed as alternatives to the semisynthetic artemisinin for the treatment of malaria[4]. They have demonstrated relatively good efficacy and low toxicity in animal studies [1,5]. Like the semisynthetic artemisinins, antimalarial ozonides form carbon-centered free radicals due to reaction of the peroxide heterocycle with heme produced by parasite hemoglobin digestion [4,6]; this is thought to account for the high antimalarial specificity of diverse classes of organic peroxides.

In addition to activity against the malarial parasite, artemisinin and its derivatives have also been shown to decrease the viability of cancer cells,[7-12] albeit at concentrations orders of magnitude greater than those required to kill malaria parasites. For example, Efferth, et al, have reported the semisynthetic artemisinin artesunate is cytotoxic to 55 National Cancer Institute cell lines [12,13] with IC₅₀'s ranging from 0.250 to \geq 100 μ M. In some instances, exposure of the cancer cell lines to semisynthetic artemisinins induces apoptosis [9,10]. However, no data have been published to date on the effects of synthetic ozonides on cancer cell lines.

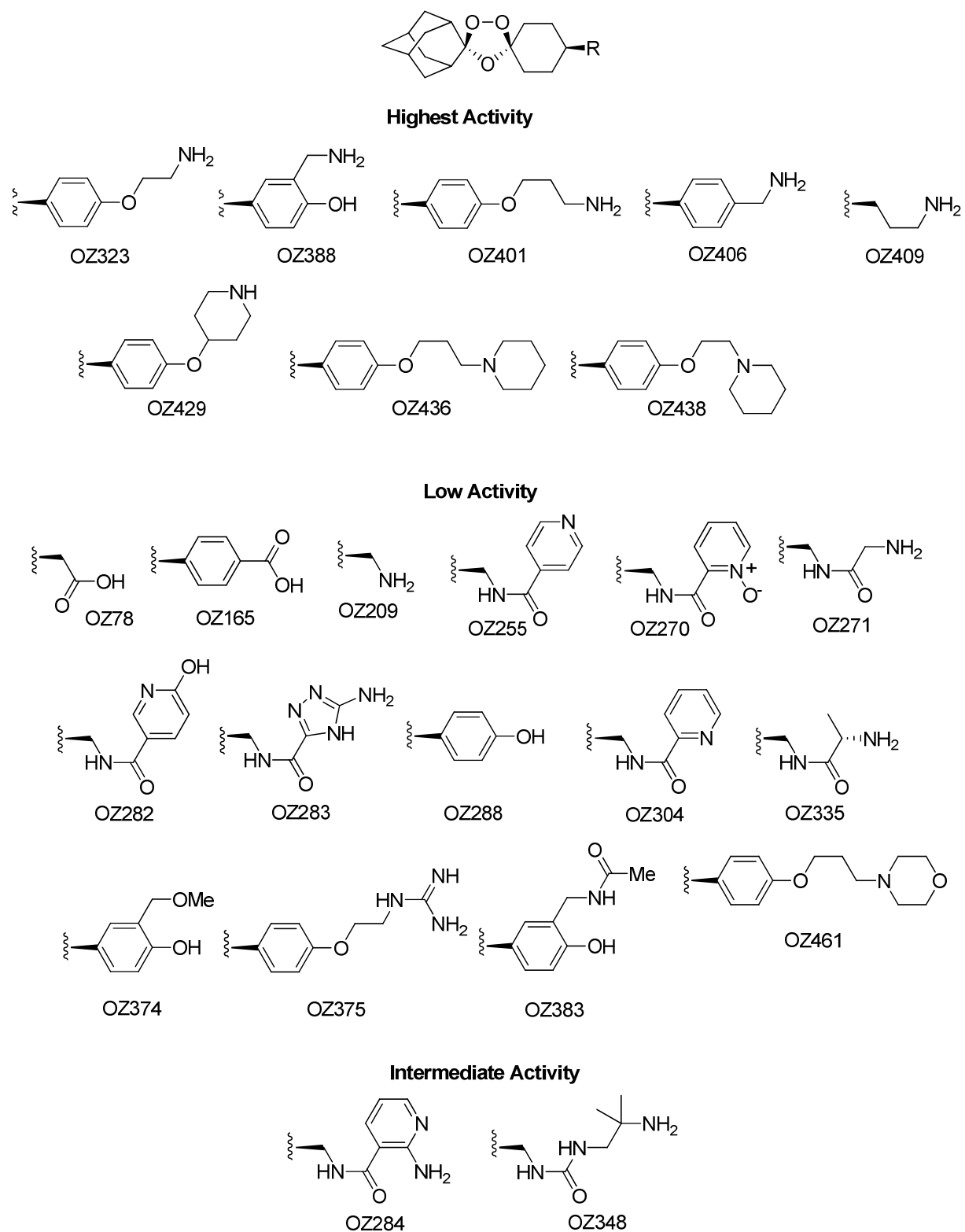


Figure 1. Ozonide structures.

The synthetic ozonides tested have four substructures: a spiroadamantane ring, a 1,2,4-trioxolane heterocycle, a 1,4-disubstituted cyclohexane ring, and an "R" group representing a wide range of functional groups (Fig. 1). In addition to the peroxide ring, the presence of both the adamantane and cyclohexane rings are required for antimalarial activity [4]. By altering the R group of the ozonides, one can relatively easily change their physicochemical and pharmacokinetic properties [14].

Using Raji human lymphoma cells as a model, we have studied the *in vitro* effect of twenty five ozonides (Fig. 1) on cell viability to determine if there were specific structural characteristics that could be used to differentiate active compounds from those with low to no activity. The compounds were separated into a set of eight highly active compounds, fifteen low activity compounds and two compounds with intermediate activity. Preliminary structure-activity relationship (SAR) studies determined the importance of an amine and an aromatic ring to decrease cell viability, but these features alone were insufficiently predictive. To better map the pharmacophore for the active compounds, molecular modeling was performed.

EXPERIMENTAL SECTION

2.1 Cell culture

Raji lymphoma cells (generously supplied by Dr. Shantaram Joshi of the Department of Genetics, Cell Biology, and Anatomy at the University of Nebraska Medical Center) were grown in T-25 flasks in RPMI 1640 media supplemented with 10% fetal calf serum (Hyclone), 2 mM L-glutamine and 100 µg/mL penicillin-streptomycin (GIBCO) at 37 °C in a humidified 5% CO₂ incubator. When cells became dense and the media started to turn slightly acidic, the cells were subcultured by removing a small volume of cell suspension (1 mL) and adding the cells to 7 mL fresh complete supplemented media.

2.2 MTT assay in 96 well plates

Raji cells growing in T-25 flasks were counted using a hemocytometer and an inverted microscope. Cells (50,000 in 100 µL fresh media) were added to each well of a 96 well plate and exposed to the experimental treatment or solvent control for 2 days unless otherwise noted. Cell viability was determined using the MTT method [15,16] similar to the conditions used by Mercer, et al [11]. After exposure to the test compounds (generously supplied by Dr. Jonathan Vennerstrom of the Department of Pharmaceutical Sciences at the University of Nebraska Medical Center), 25 µL MTT reagent (5 mg/mL 1-(4,5-dimethylthiazol-2-yl)-5-diphenylformazan in phosphate buffered saline) was added to each well and the cells were incubated for 2 hours at 37 °C. After the 2 hour incubation, 100 µL of stop solution (pH ~4.7, 50% dimethylformamide, 20% sodium dodecylsulfate, 0.5% of an 80% acetic acid/2.5% hydrochloric acid solution) was added. Cells were covered and sealed with Parafilm (Pechiney Plastic Packaging) and incubated overnight at 37 °C to dissolve the cells and the purple product. Absorbance of the purple solution was measured at 550 nm using a plate-reader spectrophotometer. All cell studies were performed at least in replicates of 6 with average background absorbance (MTT reagent in wells without cells) subtracted. Cell viability was reported as a percent absorbance relative to control cells. Control cells were exposed to the same concentration of solvent as the cells treated with test compounds. Artesunate was used in each experiment as a positive control and generally 10 µM artesunate-treated cell viability was ~30-50% that of control. Compounds were dissolved in either dimethyl sulfoxide (DMSO) or ethanol to make stock concentrations 100 times the concentration studied during the experiment.

2.3 Compound alignment and pharmacophore feature generation

Using the Protonate 3-D feature in MOE, the library of compounds (Fig. 1) was adjusted to the level of protonation that would occur at pH 7.4 and minimized using the MMFF94x forcefield [17,18]. There were three databases, one with eight highly active compounds, one with two compounds of intermediate activity, and one with fifteen compounds of low activity. The highly active compounds were aligned by their non-hydrogen atoms using the Alignment feature of MOE [17]. The energy-minimized compounds were initially aligned with the automated Rigid Body and Flexible Body alignment functions. The compounds were then aligned manually by the non-hydrogen atoms in the compounds. A pharmacophore was pursued from the aligned positively charged nitrogen and the distance to ozonide oxygen atoms.

RESULTS

3.1 Ozonides

Twenty-five ozonides were tested for their effects on the viability of Raji lymphoma cells. We initially chose R-group structures that varied greatly in their functional groups until we began to observe general structure-cell viability trends. After noticing the importance of amine functional groups, we chose compounds that had more structural similarity for further investigation.

The MTT assay was used to monitor cell viability. Cells were exposed to 10 μM concentrations of compounds. At concentrations below 10 μM , no compound measurably affected cell viability (Fig. 2). Interestingly, artesunate exhibited a more typical dose-response curve for cell viability as a function of concentration.

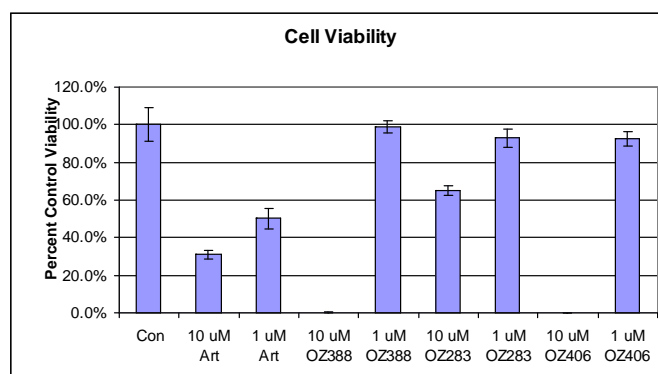


Figure 2. The effect of representative ozonides and artesunate (Art) on the viability of Raji lymphoma cells. Bars represent the average of 6 replicates plus/minus *std. dev.* using the MTT assay to measure cell viability as described in Methods

The compounds were divided into three groups based on their activity against cells exposed to 10 μM concentrations for two days. The compounds were grouped into categories of high, intermediate and low activity. Treatment with the “highly active” compounds resulted in less than 10% viable cells in all but one of 16 experiments and in most cases cell viability was less than 1%. (In one of three experiments with OZ388, viability was 28%, while the other two experiments with OZ388 viability was less than 1%.) Two compounds demonstrated intermediate activity similar to the artesunate control, with cell viability around 30-40%. The other fifteen compounds that were classified as “low activity” were less active than the artesunate in over ninety percent of paired experiments. The viability of cells treated with 10 μM of these compounds ranged from about 60 – 100% of control. The cell viability of the two intermediate activity points lies more than 2 standard deviations away from the average of each of the highly active and low activity groups of compounds. (Fig. 3).

A trend is evident with a cursory look at the structures of the highly active and low activity compounds. Five of the eight highly active compounds have a primary amine at the end of the substituent chain, while this structure is less common in the low activity compounds (5 of 15 compounds). In addition, the compounds of intermediate activity each have a primary amine. During our initial work it appeared the presence of the primary amine was a key feature in highly active compounds, but as we extended the pool of compounds, it became obvious that the relationship was more complex. The Log P/D values of the compounds were calculated (ACD Labs Log D suite software, version 7.04, Jonathan Vennerstrom, personal communication) to determine the relationship to activity. Although seven of eight highly active compounds had calculated Log P/D values greater than 5.1 while only seven of seventeen compounds with low or intermediate activity had calculated Log P/D values greater than 5.1, there is no significant trend between Log P/D values and activity (Fig. 3)..

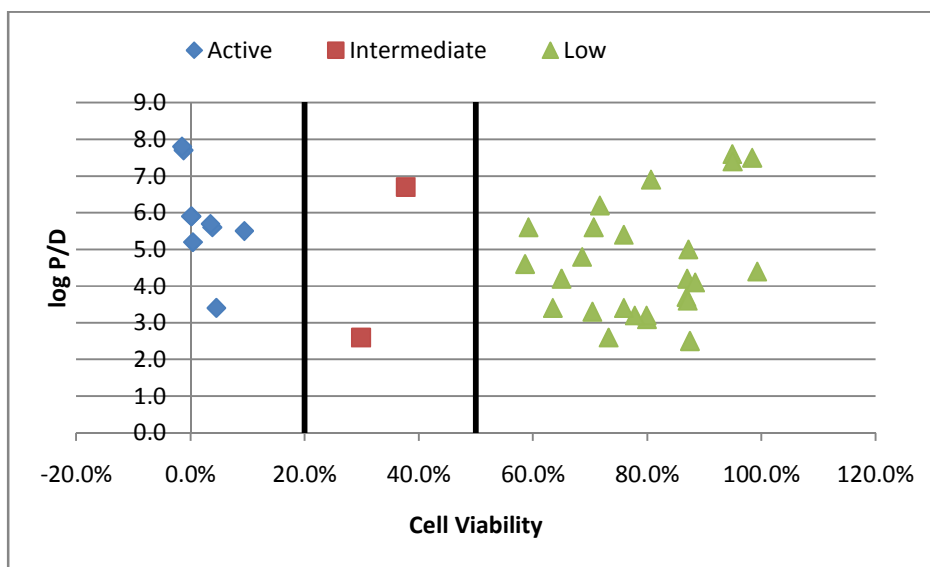


Figure 3. Calculated log P/D values do not correlate to activity of test compounds

Results clustered into the effects of active compounds and compounds with low activity while only two compounds exhibited intermediate activity. All cells were exposed to 10 μ M test compound as described in methods. Log P/D values were calculated using the ACD Labs Log D suite software, version 7.04 (personal communication, Jonathan Vennerstrom).

Although higher Log P/D values have some correlation to activity, it is insufficient to explain our results. To try to determine the structural features common to the highly active compounds we used computer modeling.

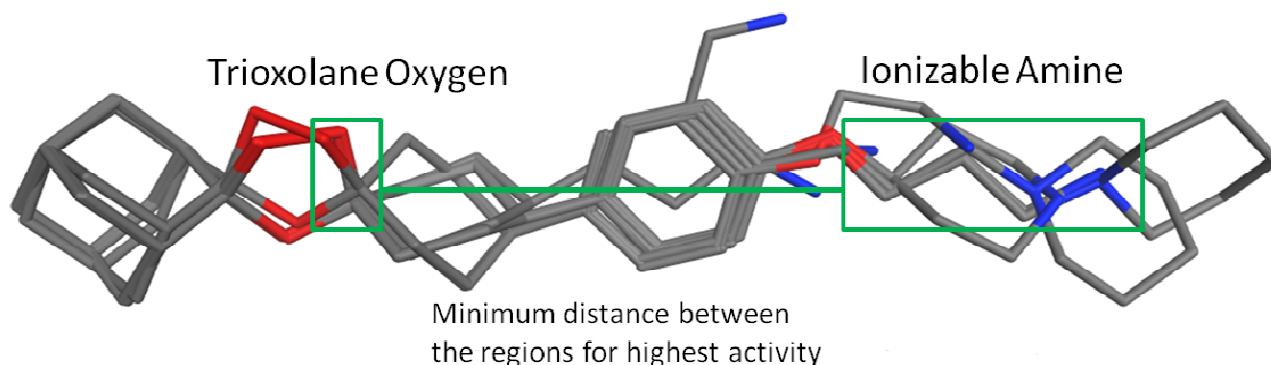


Figure 4. In this alignment image, the oxygens are red, the nitrogens are blue, the carbons are grey and the hydrogens have been omitted for clarity. The distance between the ionizable amine and the trioxolane ring required for activity is shown in Table 1.

3.2 Pharmacophore modeling

After several attempts to develop a pharmacophore for highly active compounds and perform pharmacophore conformational searches against both the highly active and low activity compound databases it was determined that the highly active compound library did not contain enough structural diversity to produce a pharmacophore. The highly active molecules did not match a search using the pharmacophore features initially developed from the automated Flexible Alignment of the highly active compound data set. Results from the alignment searches demonstrated that some highly active compounds did not match the chemical features thought to be important in the

initial development stages. Instead, manual rotation of the sigma bonds was performed to improve alignment of the nitrogens in the library to develop a new pharmacophore (see Fig. 4).

Manually rotating individual bonds in the highly active compounds produced a better alignment of the positively-charged nitrogens, while keeping the oxygen atoms in the hydrogen acceptor regions of the trioxolane aligned. OZ406 was rotated 180 degrees about its backbone, which resulted in the peroxide oxygen aligning with the ether oxygen of the other library members. The nitrogen of OZ406 was realigned to the other nitrogens in its pharmacophore region. This change in orientation effectively extended the amine group of OZ406 closer to its respective pharmacophore region (see Figure 5).

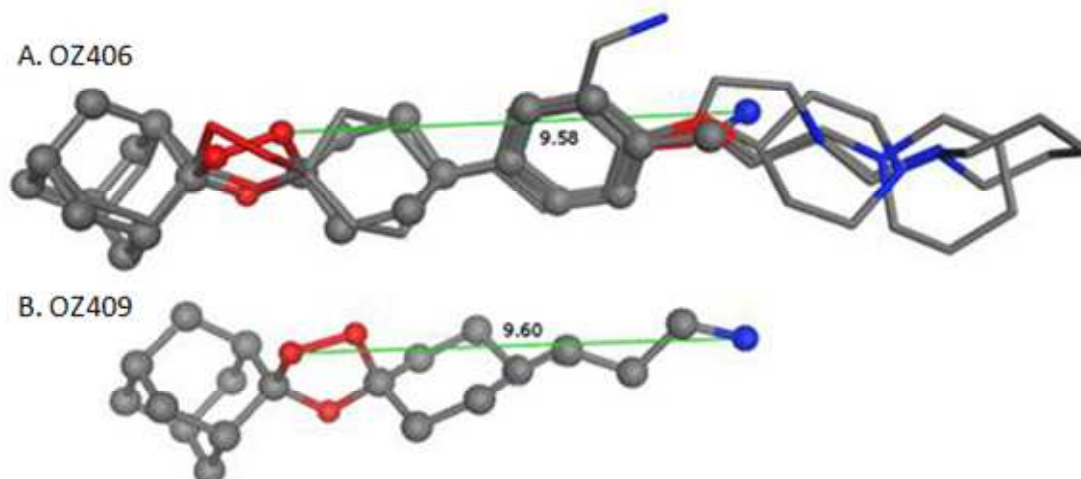


Figure 5. A. Rotation of OZ406, rendered as the ball and stick in the top set, aligned the peroxide oxygens of the library members allows the ionizable amine to fit within the putative pharmacophore region. B. OZ409's amine also projects into the putative region required for inhibiting Raji cell growth if the distal peroxide oxygen is aligned with the proximal peroxide oxygen of the other library members.

This flipped orientation for OZ406 was the only foreseeable way to place the amine in the pharmacophore region while keeping the hydrogen-acceptor regions of the trioxolane aligned. The ether oxygen and peroxide group in the trioxolane ring could be interchanged within the pharmacophore region with respect to the hydrogen accepting regions, and even shifted as seen with OZ409 in Figure 5. Ultimately, only the trioxolane ether oxygen and the peroxide oxygen proximal to the amine were necessary for determining activity *in silico*. It was also noted that any highly active compound with an oxygen bonded to a carbon in the structure's phenyl ring had naturally aligned its oxygen to those of other highly active compounds after manual bond rotation to align the amine group and trioxolane moiety oxygen atoms. This oxygen results in a secondary hydrogen acceptor region and suggested that the phenolic oxygen atom maintains some kind of interaction with the putative target, but since it is not found in all of the highly active molecules, it is not essential for activity.

Table 1. The distances between the cationic nitrogen and the trioxolane ring oxygens

| Compounds | Distance in Angstroms from the nitrogen to the <u>trioxolane non-peroxide oxygen</u> | Distance in Angstroms from the nitrogen to the <u>trioxolane proximal peroxide oxygen</u> |
|-----------|--|---|
| OZ323 | 13.05 | 9.74 |
| OZ388 | 12.34 | 8.86 |
| OZ401 | 12.32 | 8.83 |
| OZ406 | 12.51 | 9.06 |
| OZ409 | 11.83 | 8.49 |
| OZ429 | 12.81 | 9.47 |
| OZ436 | 12.72 | 9.42 |
| OZ438 | 12.47 | 9.13 |

The distances from the positively-charged nitrogen atom to the two designated oxygen atoms of the trioxolane heterocycle were measured and compared (Table 1). The average distance from the nitrogen to the trioxolane non-peroxide oxygen was 12.6 ± 0.26 angstroms and from the nitrogen to the proximal peroxide oxygen was 9 ± 0.41 angstroms.

DISCUSSION

Initial interest in these ozonides was to explore their effect on lymphoma cell viability. Compounds in the artemisinin family have been shown to be cytotoxic to cancer cells, so we investigated the effect of these ozonides on lymphoma cells. Interestingly, all of the ozonides we tested at $1 \mu\text{M}$ exhibited essentially no effects while the highly active ozonides killed more than 90% of the cells at $10 \mu\text{M}$. Thus, a subset of the ozonides is active against the cancer cell line, but at a concentration orders of magnitude higher than reported for the *in vitro* activity of these ozonides against the malarial parasite⁴. Limited dose-response curves at concentrations between 1 and $10 \mu\text{M}$ did not show intermediate effects on cell viability – either the compounds were maximally active or were inactive. However, determination of the mode of action for the effects of these compounds on cell viability was beyond the scope of this study.

The set of ozonides with the highest activity against the Raji lymphoma cells have a number of features in common. Observation of the 2-dimensional structures revealed some general features of these molecules beyond the adamantane and ozonide heterocycle. The most striking was an ionizable nitrogen that is predominately protonated at pH 7.4, usually a primary amine. The most highly active compounds also had a narrow distance range between the ionized amine and the 1,2,4-trioxolane heterocycle (defined in Table 1). In addition, all but one of the highly active compounds contained a phenyl ring between the peroxide ring and the amine. The low activity compounds were individually overlaid onto the flexibly aligned highly active compounds and their bonds rotated until similar atoms and characteristic regions overlapped with those of the highly active compounds. These conformations showed the structural differences between the highly active and low activity compounds, and gave information as to why they have low activity. Below, we discuss the features of the compounds that do not fit the model and are likely to cause them to have low activity.

A number of compounds with low activity have obvious structural differences compared to the highly active compounds; these include carboxylic acids OZ078 and OZ165, and phenols OZ288 and OZ374. The low activity of these compounds supports our hypothesis that an amine is required for activity. Another low activity compound with a partial negative charge is the N-oxide OZ270. Morpholine OZ461 is an interesting compound that is very similar to the more basic and highly active piperidines OZ436 and OZ438. The presence of the oxygen reduces the ability of the nitrogen in the morpholine to act as a base by inductively pulling electron density. This set of compounds further supports our hypothesis that a predominately ionized nitrogen is important for inhibiting the growth of the Raji cells. Compounds OZ255, OZ282, OZ283, OZ304, and OZ383 contain nitrogens, but are not predominately protonated at physiological pH. OZ283 is unionized at physiological pH because the lone pair electrons of the terminal amine are delocalized through the aromatic ring. These data support the idea that the ionization of a weak-base nitrogen is a critical component of ozonide activity against lymphomas.

OZ209 is one of the low activity compounds that contains an ionizable amine required for our model of activity. However, the core structure of OZ209 does not contain a phenyl substructure present in most of the highly active compounds. Lack of this phenyl group along with the existence of only a short carbon chain prevents OZ209 from making simultaneous contact with the hydrogen acceptor regions of the trioxolane ring and the positively charged amine region of the putative pharmacophore. OZ409 supports our hypothesis of a minimum distance requirement between the trioxolane ring and the ionizable amine since it lacks the phenyl seen in most of the compounds but does have two more methylenes than OZ209.

Amino amide OZ335 is a weakly active compound. The nitrogens that fit the pharmacophore distance necessary for activity are found in a neutral amide group, supporting our hypothesis that a nitrogen atom roughly 9 \AA away from the trioxolane moiety is not sufficient for activity unless the nitrogen is positively charged. Another low activity compound containing a nitrogen atom is OZ375 which terminates in a guanidine moiety. Under physiological conditions, the positive charge is delocalized across the three nitrogens. This data suggests that the pharmacophore for activity may be further refined to state that a static positive charge is required for activity as opposed to the

delocalized positive charge possible in other functional groups. Additional compounds would need to be tested to fully support this claim. Interestingly, although this compound is substantially less active than artesunate, it led to the lowest cell viability of all the compounds that we classified as low activity.

OZ284 and OZ348 were classified as having intermediate activity, which can be structurally explained in that they are not always in their active conformations or lowest energy conformations. These two compounds are able to adopt conformational isomers that promote the formation of an intramolecular H-bond involving the amine that may contribute to reduced activity. First, the charge stabilization provided by the H-bond reduces the positive character of the nitrogen. Since some of the compounds described above demonstrated the need for an unencumbered static positive charge for activity, then it is possible to envision a scenario where the conformation with the intramolecular H-bond is less active and supports the low activity observed by OZ271 and OZ335 since primary amines on the alpha carbon are in a favorable position for participation in an intramolecular hydrogen bond. The second factor that may contribute to a reduction in activity for these compounds could be a steric effect. One possibility that has to be considered is the distance dependence of bonding interactions. The positively charged nitrogen may be simply unable to reach the target site in a manner that would provide the optimal bonding distance.

CONCLUSION

In conclusion, a series of antimalarial ozonides were assayed in a MTT cell viability screen. Eight of the compounds were active against the Raji lymphoma cells at 10 μ M. A computational analysis of the library was performed in an effort to develop a pharmacophore that would account for the high activity of the eight members of the library. An ionizable amine was present in all of the highly active compounds, separated from the trioxolane heterocycle by a narrow distance range. Fifteen compounds had low activity and did not fit the criteria of the model. Two of the compounds appeared to have an intermediate activity that may be explained by formation of an intramolecular H-bond.

Acknowledgments

We would like to thank Jonathan L. Vennerstrom, Yuxiang Dong, and Alex Buga for their various and invaluable help, including calculation of the log P/D values. We would also like to thank the University of Nebraska at Omaha Chemistry Department.

REFERENCES

- [1] Klayman, D. L. *Science* **1985**, 228, 1049-1055.
- [2] Jefford, C. W. *Curr. Med. Chem.* **2001**, 8, 1803-1826.
- [3] Cumming, J. N.; Ploypradith, P.; Posner, G. H. *Adv. Pharmacol.* **1997**, 37, 253-297.
- [4] Vennerstrom, J. L., et al *Nature* **2004**, 430, 900-904.
- [5] Padmanilayam, M.; Scoreaux, B.; Dong, Y.; Chollet, J.; Matile, H.; Charman, S. A.; Creek, D. J.; Charman, W. N.; Tomas, J. S.; Scheurer, C.; Wittlin, S.; Brun, R.; Vennerstrom, J. L. *Bioorg. Med. Chem. Lett.* **2006**, 16, 5542-5545.
- [6] Tang, Y.; Dong, Y.; Wang, X.; Sriraghavan, K.; Wood, J. K.; Vennerstrom, J. L. *J. Org. Chem.* **2005**, 70, 5103-5110.
- [7] Epstein, M. A.; Achong, B. G.; Barr, Y. M.; Zajac, B.; Henle, G.; Henle, W. *J. Natl. Cancer Inst.* **1966**, 37, 547-559.
- [8] Woerdenbag, H. J.; Moskal, T. A.; Pras, N.; Malingre, T. M.; el-Feraly, F. S.; Kampinga, H. H.; Konings, A. W. *J. Nat. Prod.* **1993**, 56, 849-856.
- [9] Singh, N. P.; Lai, H. C. *Anticancer Res.* **2004**, 24, 2277-2280.
- [10] Nam, W.; Tak, J.; Ryu, J. K.; Jung, M.; Yook, J. I.; Kim, H. J.; Cha, I. H. *Head & Neck* **2007**, 29, 335-340.
- [11] Mercer, A. E.; Maggs, J. L.; Sun, X. M.; Cohen, G. M.; Chadwick, J.; O'Neill, P. M.; Park, B. K. *J. Biol. Chem.* **2007**, 282, 9372-9382.
- [12] Efferth, T. *Drug Resist Updat* **2005**, 8, 85-97.
- [13] Efferth, T.; Dunstan, H.; Sauerbrey, A.; Miyachi, H.; Chitambar, C. R. *Int. J. Oncol.* **2001**, 18, 767-773.
- [14] Dong, Y., et al *J. Med. Chem.* **2005**, 48, 4953-4961..
- [15] Mosmann, T. *J. Immunol. Methods* **1983**, 65, 55-63
- [16] Hansen, M. B.; Nielsen, S. E.; Berg, K. *J. Immunol. Methods* **1989**, 119, 203-210.
- [17] Chemical Computing Group **2010**, .

[18] Halgren, T. A. *Journal of Computational Chemistry* **1996**, 17, 490-519.